Optics & Laser Technology 90 (2017) 185–189

Contents lists available at ScienceDirect

Optics & Laser Technology

journal homepage: www.elsevier.com/locate/optlastec

Full length article

Quasi-three-level orthogonally polarized cw dual-wavelength operation in $Nd:LiYF_4$

Jing Zhang[a,*], Jing Xia[b], Xihong Fu[c], Pei Zhai[c]

[a] School of Science, Changchun University of Science and Technology, Changchun 130022, China
[b] School of Physical Science and Technology, Yunnan University, Kunming 650091, China
[c] Laboratory of Optical System Advanced Manufacturing Technology, Changchun Institute of Optics, Fine Mechanics and Physics, Chinese Academy of Sciences, Changchun 130033, China

ARTICLE INFO

Keywords:
Dual-wavelength
Orthogonally polarized laser
Quasi-three-level
Nd:YLF crystal

ABSTRACT

A diode-end-pumped quasi-three-level orthogonally polarized continuous-wave (cw) dual-wavelength $Nd:LiYF_4$ (Nd:YLF) laser that generates simultaneous laser at the wavelengths 903 nm and 908 nm was demonstrated. Two types of cavity configurations were studied to support the stable dual-wavelength operation of the laser. A polarization beam splitter (PBS) was placed in the first type of cavity to split the beams polarizing in two orthogonal directions. At an absorbed pump power of 21.4 W, the cw output power obtained at 903 nm in π-polarization and 908 nm in σ-polarization is 0.43 W and 3.31 W, respectively. Furthermore, in order to balance the gain-to-loss, an uncoated glass plane was inserted in the second type of cavity. By adjusting the inclination of the glass plane relative to the optical axis of the resonator, we realized the stable simultaneous dual-wavelength operation. The cw output powers of 1.82 W at 903 nm and of 2.92 W at 908 nm were obtained.

1. Introduction

In recent years, dual-wavelength laser is a hotter research topic internationally. It is used extensively in interference rainbow holograph [1], fine laser spectrum [2], differential absorption radar [3], nonlinear frequency conversion [4], laser medicine and so on [5]. All solid-state dual-wavelength lasers are more and more important, because its structure is impact and can be miniaturized, and it is able to supply more output power, and can cover wider band. Because Neodymium ion doped laser crystal has high-gain, good thermal and mechanical properties, it is now the most important gain media of all solid-state dual-wavelength lasers. Nd^{3+} doped laser crystal has three main transition lines: $^4F_{3/2}\rightarrow{}^4I_{9/2}$, $^4F_{3/2}\rightarrow{}^4I_{11/2}$, and $^4F_{3/2}\rightarrow{}^4I_{13/2}$. Currently there are mainly two types of all solid-state dual-wavelength lasers. The first type is dual-wavelength laser with bigger wavelength spacing, the lasing wavelengths of which are mainly from the two of three transition lines of Neodymium-doped laser crystal. Because the wavelength spacing of dual-wavelength laser is bigger, we can rationally design the membrane system of output coupling system of resonator to balance the gain and loss of dual wavelengths, so that to satisfy the threshold condition of simultaneous oscillation of dual wavelengths [6]. By using this method of optimizing membrane system of output coupling system and combining the simple two-mirror linear cavity structure, dual-wavelength laser output with bigger wavelength spacing has been realized in Nd:YAG [7–9], $Nd:YVO_4$ [10,11], $Nd:GdVO_4$ [12–14] and $Nd:YAO_3$ [15,16] laser. This method relies on the membrane system of output system, while it's very difficult for practical film coating to reach the theoretical expectation. Some uses complex cavity to oscillate dual wavelengths in their respective independent sub-cavities, and changes the intracavity power density and mode-matching condition by adjusting cavity lengths, so that to balance gain and loss of dual wavelengths and realize simultaneous dual-wavelength operation [10,17]. But when separating dual wavelengths, film coating technique is also needed for beam splitter. The second type is dual-wavelength laser with smaller wavelength spacing. Dual-wavelength operation of this type of laser is resulted by the splitting of stark levels of a transition line of Nd-doped laser crystal. Since the wavelength interval is very small (< 10 nm), utilizing current coating technique for separation is very difficult. Actually, even if the coating parameters can reach the pre-calculated theoretical values, simultaneously dual-wavelength oscillation is difficult to obtain because of the uncertain other parameters of the laser. So far there are mainly two approaches to make this kind of dual-wavelength laser. The first approach is to insert some element inside the cavity and use the element's different characteristics for dual wavelengths to balance their gain-to-loss. For example, H. H. Yu et al. inserted Gr:YAG crystal inside

Abbreviations: PBS, polarization beam splitter; HT, high transmission; HR, high reflectivity; TEC, thermal electronic cooled

* Corresponding author.
E-mail address: optics@sina.cn (J. Zhang).

http://dx.doi.org/10.1016/j.optlastec.2016.09.002
Received 18 May 2016; Received in revised form 25 July 2016; Accepted 1 September 2016
Available online 09 December 2016
0030-3992/

the cavity, and utilized its different absorption characteristics for different wavelengths to obtain the gain-to-loss balance of dual wavelengths. With this approach, they realized 1052 nm, 1064 nm and 1061 nm, 1059 nm dual-wavelength outputs in Nd:YAG [18] and Nd:CNGG [19] lasers respectively. With the same method, H.T. Huang et al. inserted V:YAG crystal inside the cavity, which helps realizing 932.9 nm and 936.5 nm dual-wavelength output in Nd:GGG [20] laser respectively. We inserted Lyot filter inside the cavity, and realized 884 nm and 885 nm dual-wavelength output in 885 nm qusi-three-level Nd:YAG laser by adjusting the free spectral range of Lyot filter [21]. Moreover, in some Nd-doped laser crystals, the emission cross sections of the two transition wavelengths from some Stark energy level splits are close. Thus, in realizing one transition wavelength operation caused by a Stark split, if we don't take any measures, the other wavelength would also oscillate [22–26]. Beams of dual wavelengths with small interval realized by the method above always have the same polarization. The second method is using polarization beam splitter or F-P etalon with a tilt angle to separate the two wavelength beams with orthogonal polarizations and keep them oscillating in their own cavities. Then the membrane system of each cavity's output mirror is designed to balance gain-to-loss of dual wavelengths, so that the thresholds of dual wavelengths can be equalized [27–31]. This kind of small interval orthogonal polarization dual-wavelength laser beam can realize coherent THz with 0.1–3 Hz frequency range [32], which has a great potential application in THz imaging, THz remote sensing [33], THz spectroscopy [34,35], laser interferometer [36] and precision metrology [37].

Research on 900 nm Nd^{3+} doped solid state laser operating at quasi-three level is an important part in all solid state laser research field. The laser at this waveband can be extensively applied in laser remote sensing, laser satellite work, laser communication, etc. Moreover, after the intra-cavity or extra-cavity frequency doubling, the blue laser from it has very extensive application and promising future in high intensity storage, ultra-short pulse, digital video technology, spectrum technology, laser medicine, large screen laser displays, marine military application and underwater resource detection, etc.

Among the various Nd^{3+}-doped crystals, Nd:YLF is one of the most widely studied laser crystals in the literature. It is a crystal that brings some interesting attributes to solid state lasers, such as weak negative thermal lensing and different laser wavelengths. Nd:YLF is a naturally birefringent crystal which overwhelms any thermally-induced birefringence, guarantying a polarized laser emission. As we know, there exist three transitions: ${}^4F_{3/2}\rightarrow{}^4I_{11/2}$, ${}^4F_{3/2}\rightarrow{}^4I_{13/2}$ and ${}^4F_{3/2}\rightarrow{}^4I_{9/2}$ in Nd^{3+}. For four-level Nd:YLF laser corresponds to ${}^4F_{3/2}\rightarrow{}^4I_{11/2}$ and ${}^4F_{3/2}\rightarrow{}^4I_{13/2}$ transitions. In ${}^4F_{3/2}\rightarrow{}^4I_{11/2}$ transition, when gain is maximum, 1047 nm π-polarization emission is output [38,39]. After applying measures of frequency selection, 1053 nm σ-polarization emission can be obtained [40,41]. In ${}^4F_{3/2}\rightarrow{}^4I_{13/2}$ transition, single wavelength output of 1321 nm [42,43] or 1313 nm [44,45] around 1.3 µm has been reported. The quasi-three level emission spectral line of Nd:YLF laser is corresponding to ${}^4F_{3/2}\rightarrow{}^4I_{9/2}$ transition. The transition of the ${}^4F_{3/2}$ level to the ground state delivers laser emissions at 903 nm for π-polarization and 908 nm for σ-polarization (see Fig. 1). Because of the Stark energy split of Nd:YLF crystal field, the ground state is split into five fine structures. At room temperature, the particle population of Z_5 energy is about 3.4% of total number of particles, while for 946 nm quasi-three level Nd:YAG, the particle population of Z_5 energy is about 0.74% of total number of particles [46]. So the threshold of quasi-three level Nd:YLF laser is higher than that of quasi-three level Nd:YAG laser. Moreover, in quasi-three level laser, the reabsorption of lower level is very evident, which increases the difficulty of laser generation. 903 nm [47] or 908 nm [48,49] single wavelength output has already been demonstrated, but (1047 nm and 1053 nm), (1321 nm and 1313 nm) or (903 nm and 908 nm) dual-wavelength simultaneous output has never been reported so far.

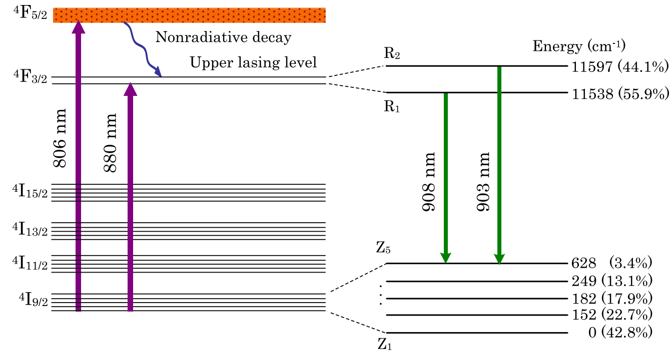

Fig. 1. Nd:YLF energy level scheme at 300 K with the main pump and emission transitions.

In this work, we will present our recent results of exploring a dual-wavelength Nd:YLF laser. By separating the orthogonally polarized beams with a PBS, the dual-wavelength Nd:YLF laser operation was realized at two wavelengths of 903 nm and 908 nm. At an absorbed pump power of 21.7 W, the output powers of 0.36 W at 903 nm and of 2.75 W at 908 nm are simultaneously obtained. Moreover, an uncoated glass plane was inserted in the laser cavity. By adjusting the inclination of the glass plane, we realized the stable simultaneous output power obtained at 903 nm and 908 nm is 1.55 W and 2.28 W, respectively.

2. Experiment and analysis

In order to obtain an orthogonally polarized dual-wavelength laser beam, we designed the first type of cavity configuration as shown in Fig. 2. The optical pumping was done by using fiber-coupled (diameter of 200 µm and numerical aperture NA=0.22) diode lasers from Coherent Co., USA. The 806 nm emitting diode outputted 30 W of pump power with an emission bandwidth of 2.5 nm (FWHM definition). The coupling optics consists of two identical plano-convex lenses with focal lengths of 15 mm used to re-image the pump beam into the laser crystal at a ratio of 1:1. The coupling efficiency is 95%. The laser crystal is a 1.0 at% Nd^{3+} doped, 3 mm×3 mm×5 mm Nd:YLF wrapped with indium foil and mounted at a TEC (thermal electronic cooled) copper block, and the temperature is maintained at 20 °C. The whole cavity is also cooled by TEC. Both sides of the laser crystal were coated for high transmission (HT) from 900 to 910 nm. A PBS was placed in the cavity to split the beams polarizing in two orthogonal directions. The concave mirror, M1, with a radius of curvature −100 mm was used as the input coupler, which was coated for high reflectivity (HR) at 903 and 908 nm and HT at 806 nm, and HT at 1047, 1053, 1313 and 1321 nm to suppress the strong parasitical oscillation at these transitions. The plane mirror, M2, was used as the output coupler for π-polarized. The concave mirror, M3, was used as the output coupler for σ-polarized.

For a diode-pumped solid-state quasi-three-level laser, the threshold condition for each transition wavelength in a cw simultaneous dual-wavelength operation is given by [50]

$$P_{th,i} = \frac{\ln(1/R_i) + L_i + 2\sigma_i l f_a N_0}{2l\eta_{Qi} f_{bi}} \frac{h\nu_p}{\sigma_i \tau_i} \frac{1}{\iiint s_i(r, z) r_p(r, z) dv}, \tag{1}$$

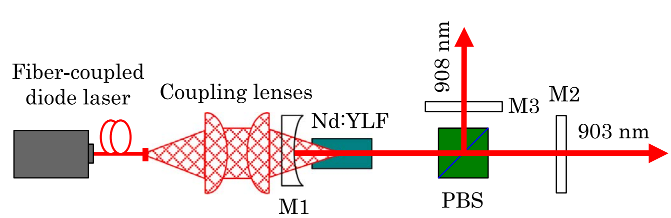

Fig. 2. The first type of cavity configuration for the diode-pumped Nd:YLF dual-wavelength laser.

where R_i is the reflectivity of the output coupler, L_i is resonator round-trip residual losses at the corresponding transition wavelength, l is the length of the active medium, η_{Qi} the quantum efficiency, f_a is the fraction of the $^4I_{9/2}$ population that resides in the Stark component used as the lower laser level, f_{bi} is the fraction of the $^4F_{3/2}$ population that resides in the Stark component used as the upper laser level. τ_i is the fluorescence lifetime at the upper level, η_{Qi} is the quantum efficiency for the corresponding transition, σ_i the stimulated emission cross section, N_0 is the total dopant concentration, $h\nu_p$ is the pump photon energy, $s_i(r, z)$ is the normalized cavity mode intensity distribution for the corresponding transition, and $r_p(r, z)$ is the normalized pump intensity distribution in the active medium. Here i=1, 2 represents the two wavelengths of 903 nm and 908 nm, respectively. The ratio of laser thresholds for 903 nm and 908 nm can be expressed as:

$$\beta = \frac{\ln(1/R_2) + L_2 + 2\sigma_2 l f_a N_0}{\ln(1/R_1) + L_1 + 2\sigma_1 l f_a N_0}\cdot\frac{f_{b1}\sigma_1}{f_{b2}\sigma_2}\cdot\frac{\iiint s_1(r, z) r_p(r, z) dv}{\iiint s_2(r, z) r_p(r, z) dv} \quad (2)$$

The basic parameters used in the experiment are $\sigma_1=1.2\times10^{-20}$ cm^2, $\sigma_2=1.3\times10^{-20}$ cm^2, f_a=0.13, f_{b1}=0.44, f_{b2}=0.56, l=8 mm, $N_0=1.4\times10^{20}$ cm^3, $L_1=L_2$=0.005. The values of L_i were measured by the Findlay–Clay method [51]. With Eq. (2) and the parameters, if we assumed that R_1 for 903 nm was 99.0%, R_2 for 908 nm must be 96.2% to satisfy the dual-wavelength oscillation condition, i.e. β=1. The measured reflectivities of the output mirrors are 99.4% and 96.2% at 903 nm and 908 nm respectively in our experiment.

Fig. 3 shows the output power at each lasing wavelength with respect to the absorbed pump power at 806 nm. At an absorbed pump power of 21.4 W, the cw output power obtained at 903 nm and 908 nm is 0.43 W and 3.31 W, respectively. A total output power of 3.74 W for the dual-wavelength was achieved with optical conversion efficiency of 17.5%. The threshold pump power is 7.2 W for 903 nm, and 10.3 W for 908 nm, respectively. Further analysis showed the reason why thresholds are different was the feedback difference between the π-polarization and σ-polarization, which was caused by the output coupler. In fact, the experimental reflection of M2 (R_2=99.4%) is bigger than the theoretical reflection of 99.0% derived by Eq. (2), which results $\beta > 1$. The result of $\beta > 1$ means that the laser will first emit the radiation at the weaker line at 903 nm and then emit the radiation at 908 nm under a higher pump power. It can be seen from Fig. 3 that the output power of 908 nm line increases monotonically as the pump power increases. On the other hand, the output power of 903 nm line first increases linearly with the pump power, reaches its maximum power of 1.21 W at the pump power of 17.2 W, and then descends monotonically. We believe that the gain competition between 903 nm and 908 nm lines leads to the output power of 903 nm decreases over 17.2 W of pump power. The laser beams were observed at different pump powers. The M^2 factor of 903 nm emission is estimated to be approximately 1.12 near threshold, and then increases to 2.32 at pump power greater than

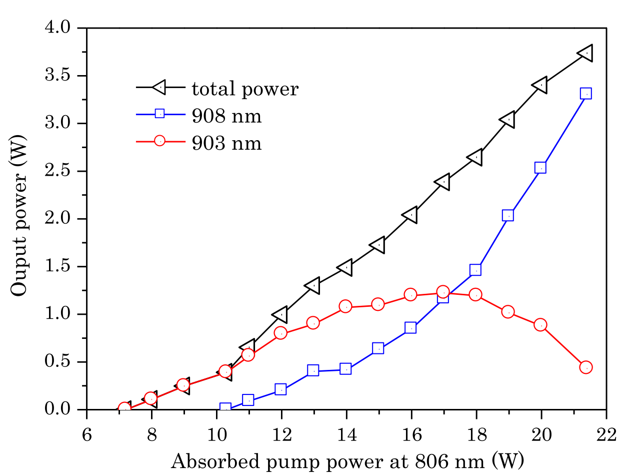

Fig. 3. Output powers versus the absorbed pump power for dual-wavelength operation.

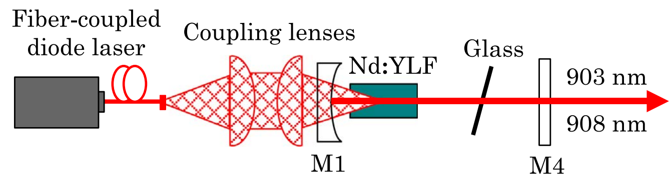

Fig. 4. The second type of cavity configuration for the diode-pumped Nd:YLF dual-wavelength laser.

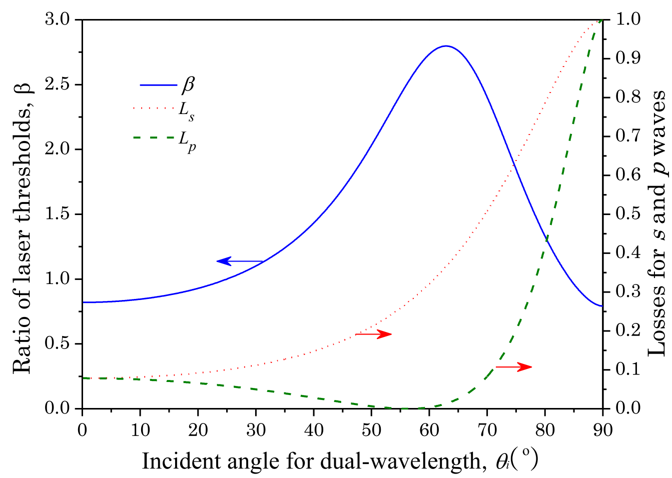

Fig. 5. Dependence of the ratio of laser thresholds and the relative losses for s and p waves on the incident angle for dual-wavelength.

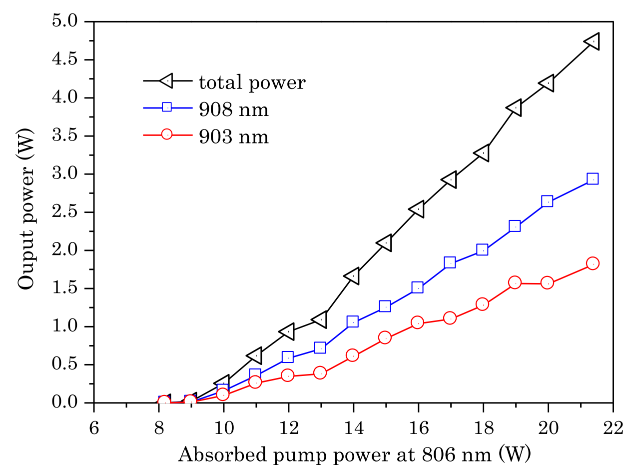

Fig. 6. Output powers versus the absorbed pump power for dual-wavelength operation.

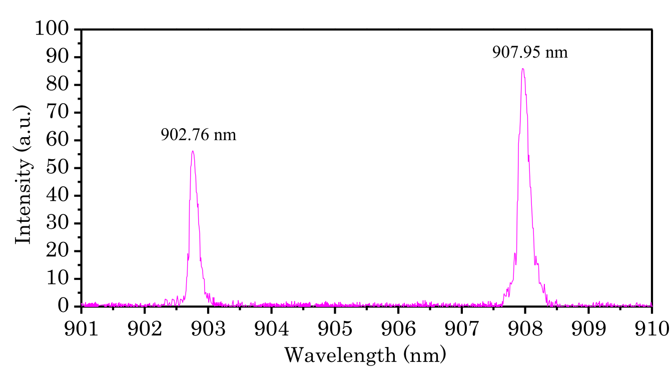

Fig. 7. Optical spectrum of dual-wavelength operation.

21.4 W. On the other hand, the 908 nm emission maintains the beam quality factor M^2 less than 1.08 over the full range of pump powers. The stability testing is carried out by monitoring the output powers of each wavelength with a Field-Master-GS powermeter at 10 Hz. The fluctuations for 908 nm and 903 nm lights at the pump power of 21.4 W are about 3.5% and 5.3% in 4 h, respectively.

Because the laser output from the first type of cavity configuration featured two beams, it is sometimes inconvenient for applicants though the beams can be easily recombined using reflectors and PBS. To improve this, the second type of cavity configuration featuring one beam output was presented as shown in Fig. 4. The pump source, the gain medium, the coupling lenses and the input mirror were the same as the corresponding ones in the first type of cavity configuration mentioned above. An uncoated glass plate with a thickness of 0.5 mm was inserted in the cavity. The plane mirror, M4, was used as the output coupler, which was coated with transmission of 2.3% from 900 nm to 910 nm. The cavity length was approximately 20 mm.

Since $f_{b1} < f_{b2}$, $\sigma_1 < \sigma_2$, $R_1 \approx R_2$ and the two nearly close wavelengths in the same cavity, the ratio β is less than 1 without introducing the deliberate difference for losses L_1 and L_2. The result of $\beta < 1$ indicates that the laser will be dominated at 908 nm because this emission line has a lower threshold. For obtaining a dual-wavelength simultaneous operation, an appropriate difference for losses L_1 and L_2 needs to be introduced to reach the condition of β=1. The single pass losses caused by the Fresnel reflection for s and p waves can be given by [52]

$$L_s = \left|\frac{\sin(\theta_i - \theta_t)}{\sin(\theta_i + \theta_t)}\right|^2 + \left[1 - \left|\frac{\sin(\theta_i - \theta_t)}{\sin(\theta_i + \theta_t)}\right|^2\right] \cdot \left|\frac{\sin(\theta_t - \theta_i)}{\sin(\theta_t + \theta_i)}\right|^2 \tag{3}$$

$$L_p = \left|\frac{\tan(\theta_i - \theta_t)}{\tan(\theta_i + \theta_t)}\right|^2 + \left[1 - \left|\frac{\tan(\theta_i - \theta_t)}{\tan(\theta_i + \theta_t)}\right|^2\right] \cdot \left|\frac{\tan(\theta_t - \theta_i)}{\tan(\theta_t + \theta_i)}\right|^2, \tag{4}$$

where θ_i is the inclined angle of the glass plane (equal to the incident angle of light), θ_t is the refractional angle of light, and $\sin\theta_i = n\sin\theta_t$, n(=1.5) is the refractive index of the glass plane.

It can be seen in Fig. 5 that the overlapping curves for the single pass losses L_s and L_p at the small incident angle, and then gradually separate. In our experiment, the σ-polarization of Nd:YLF crystal is set to be placed in the parallel direction, and the angle of inclination of the glass plane is relative to the optical axis of the resonator, which the plane of incidence is in the horizontal direction. As a result, the σ- and π-polarized waves are perpendicularly and parallel to the plane of incidence, corresponding to the s and p waves respectively. Substituting Eqs. (3) and (4) into Eq. (2), the ratio of laser thresholds β are calculated as a function of incident angle θ_i and the result was shown in Fig. 5. As shown in Fig. 5, the ratio of laser thresholds β increases with the incident angle θ_i, reaches a maximum, and then falls with further increase in the incident angle. In our experiment, we will control the incident angle θ_i to be approximately 25° to obtain a ratio of $\beta \approx 1$.

The output powers at each lasing wavelength versus absorbed pump power are given in Fig. 6. It can be seen that the output powers of both wavelengths monotonically increased as the pump power increased. When the absorbed pump power was increased to about 8.2 W, the dual-wavelength radiation was emitted. According to the experimental results, as the absorbed pump power was increased, the 903 nm transition was not suppressed by the 908 nm transition. The cw output power obtained at 903 nm and 908 nm was 1.82 W and 2.92 W, respectively. A total output power of 4.74 W for the dual-wavelength was achieved at the absorbed pump power of 21.4 W with optical conversion efficiency of 22.1%. The fluctuations for 908 nm and 903 nm lights at the pump power of 21.4 W are about 2.1% and 2.3% in 4 h, respectively. We also found that the fluctuations in the output powers of each wavelength were substantially reduced. We believe that the competitive interaction between two wavelengths is due to the gain-to-loss balances. The M^2 values for 903 nm and 908 nm lights at the pump power of 21.4 W were found to be around 1.13 and 1.15, respectively. Using the LABRAM-UV spectrum analyzer to scan the dual-wavelength laser and dealing with the data with software, the spectrum of the dual-wavelength laser at the pump power of 21.4 W is shown in Fig. 7. The central wavelengths are 902.76 nm and 907.95 nm, with the spectral line widths of 0.32 nm and 0.34 nm, respectively.

3. Conclusion

In conclusion, the use of diode-end-pumped Nd:YLF crystal to achieve the quasi-three-level orthogonally polarized dual-wavelength Nd:YLF laser operation at 903 nm and 908 nm has been demonstrated for the first time. Two types of cavity configuration are used to achieve simultaneous emission of two orthogonally polarized wavelengths. A PBS was placed in the first type of cavity to split the beams polarizing in two orthogonal directions. At an absorbed pump power of 21.4 W, the cw output power obtained at 903 nm and 908 nm is 0.43 W and 3.31 W, respectively. Furthermore, an uncoated glass plane was placed in the second type of cavity, and further we have numerically analyzed the condition of gain-to-loss balance via an uncoated glass plane for achieving the orthogonally polarized dual-wavelength operation. The stable cw output power obtained at 903 nm and 908 nm was 1.82 W and 2.92 W, respectively.

Acknowledgments

This work was supported by the National Natural Science Foundation of China (Grant nos. 61108029 and 61275135) & twelfth five-year scientific and technical research program of the Education Department of Jilin province of China (Grant no. 2013jyt13).

References

[1] F. Weigl, A generalized technique of two-wavelength, nondiffuse holographic interferometry, Appl. Opt. 10 (1971) 187–192.
[2] N.G. Basov, M.A. Gubin, V.V. Nikitin, A.V. Nikuchin, V.N. Petrovskii, E.D. Protsenko, D.A.Tyurikov, Highly-sensitive method of narrow spectral-line separations, based on the detection of frequency resonances of a 2-mode gas-laser with non-linear absorption, Izv. Akad. Nauk SSSR, Ser. Fiz. 46, 1982, pp. 1573–1583
[3] R.W. Farley, P.D. Dao, Development of an intracavity-summed multiple-wavelength Nd:YAG laser for a rugged, solid-state sodium lidar system, Appl. Opt. 34 (1995) 4269–4273.
[4] Y.F. Chen, Y.S. Chen, S.W. Tsai, Diode-pumped Q-switched laser with intracavity sum frequency mixing in periodically poled KTP, Appl. Phys. B. 79 (2004) 207–210.
[5] S.N. Son, J.J. Song, J.U. Kang, C.S. Kim, Simultaneous second harmonic generation of multiple wavelength laser outputs for medical sensing, Sensors 11 (2011) 6125–6130.
[6] H.Y. Shen, R.R. Zeng, Y.P. Zhou, G.F. Yu, C.H. Huang, Z.D. Zeng, W.J. Zhang, Q.J. Ye, Simultaneous multiple wavelength laser action in various neodymium host crystals, IEEE J. Quantum Electron. 27 (1991) 2315–2318.
[7] C. Bethea, Megawatt power at 1.318μ in Nd3+:YAG and simultaneous oscillation at both 1.06 and 1.318μ, IEEE J. Quantum Electron. 9 (1973) (254-254).
[8] K. Gallo, G. Assanto, All-optical diode based on second-harmonic generation in an asymmetric waveguide, J. Opt. Soc. Am. B 16 (1999) 267–269.
[9] C. Ren, S. Zhang, Diode-pumped dual-frequency microchip Nd: YAG laser with tunable frequency difference, J. Phys. D: Appl. Phys. 42 (2009) 155107(1)–155107(6).
[10] Y.F. Chen, cw dual-wavelength operation of a diode-end-pumped Nd:YVO4 laser, Appl. Phys. B 70 (2000) 475–478.
[11] Y.Y. Lin, S.Y. Chen, A.C. Chiang, R.Y. Tu, Y.C. Huang, Single-longitudinal-mode, tunable dual-wavelength, CW Nd:YVO4 laser, Opt. Express 14 (2006) 5329–5334.
[12] E. Herault, F. Balembois, P. Georges, 491 nm generation by sum-frequency mixing of diode pumped neodymium lasers, Opt. Express 13 (2005) 5653–5661.
[13] L. He, J. Du, J. Sun, S. Liu, Y.X. Fan, H.T. Wang, L.H. Zhang, Y. Hang, High efficiency single- and dual-wavelength Nd: GdVO4 lasers pumped by a fiber-coupled diode, Appl. Phys. B 79 (2004) 301–304.
[14] K. Lünstedt, N. Pavel, K. Petermann, G. Huber, Continuous-wave simultaneous dual-wavelength operation at 912 nm and 1063 nm in Nd:GdVO4, Appl. Phys. B 86 (2007) 65–70.
[15] H.Y. Shen, R.R. Zeng, Y.P. Zhou, G.F. Yu, C.H. Huang, Z.D. Zeng, W.J. Zhang, Q.J. Ye, Comparison of simultaneous multiple wavelength lasing in various neodymium host crystals at transitions from 4 F 3/2–4 I 1 1/2 and 4 F 3/2–4 I 1 3/

2, Appl. Phys. Lett. 56 (1990) 1937–1938.
[16] C.H. Huang, G. Zhang, Y. Wei, L.X. Huang, H.Y. Zhu, A Q-switched Nd:YAlO3 laser emitting 1080 and 1342nm, Opt. Commun. 281 (2008) 3820–3823.
[17] Y.F. Chen, S.W. Tsai, S.C. Wang, Y.C. Huang, T.C. Lin, B.C. Wong, Efficient generation of continuous-wave yellow light by single-pass sum-frequency mixing of a diode-pumped Nd:YVO_4 dual-wavelength laser with periodically poled lithium niobate, Opt. Lett. 27 (2002) 1809–1811.
[18] H. Yu, H. Zhang, Z. Wang, J. Wang, Y. Yu, X. Zhang, R. Lan, M. Jiang, Dual-wavelength neodymium-doped yttrium aluminum garnet laser with chromium-doped yttrium aluminum garnet as frequency selector, Appl. Phys. Lett. 94 (2009) 041126(1)–041126(3).
[19] H. Yu, H. Zhang, Z. Wang, J. Wang, Y. Yu, Z. Shi, X. Zhang, M. Jiang, High-power dual-wavelength laser with disordered Nd:CNGG crystals, Opt. Lett. 34 (2009) 151–153.
[20] H.T. Huang, J.L. He, B.T. Zhang, J.F. Yang, J.L. Xu, C.H. Zuo, X.T. Tao, V^{3+}:YAG as the saturable absorber for a diode-pumped quasi-three-level dual-wavelength Nd:GGG laser, Opt. Express 18 (2010) 3352–3357.
[21] Y. Lü, L. Zhao, P. Zhai, J. Xia, S. Li, X. Fu, Quasi-three-level neodymium-doped yttrium aluminum garnet laser emitting at 885 nm, Opt. Lett. 37 (2012) 3177–3179.
[22] Y. Lu, B.G. Zhang, E.B. Li, D.G. Xu, R. Zhou, X. Zhao, F. Ji, T.L. Zhang, P. Wang, J.Q. Yao, High-power simultaneous dual-wavelength emission of an end-pumped Nd:YAG laser using the quasi-three-level and the four-level transition, Opt. Commun. 262 (2006) 241–245.
[23] H.Y. Zhu, G. Zhang, C.H. Huang, Y. Wei, L.X. Huang, A.H. Li, Z.Q. Chen, 1318.8 nm/1338.2 nm simultaneous dual-wavelength Q-switched Nd:YAG laser, Appl. Phys. B. 90 (2008) 451–454.
[24] R. Zhou, B. Zhang, X. Ding, Z. Cai, W. Wen, P. Wang, J. Yao, Continuous-wave operation at 1386 nm in a diode-end-pumped Nd:YVO_4 laser, Opt. Express 13 (2005) 5818–5824.
[25] R. Zhou, E.B. Li, B.G. Zhang, X. Ding, Z.Q. Cai, W.Q. Wen, P. Wang, J.Q. Yao, Simultaneous dual-wavelength CW operation using $^4F_{3/2}$–$^4I_{13/2}$ transitions in Nd:YVO_4 crystal, Opt. Commun. 260 (2006) 641–644.
[26] Y.F. Chen, M.L. Ku, K.W. Su, High-power efficient tunable Nd:$GdVO_4$ laser at 1083 nm, Opt. Lett. 30 (2005) 2107–2109.
[27] C. Ren, S. Zhang, Diode-pumped dual-frequency microchip Nd: YAG laser with tunable frequency difference, J. Phys. D: Appl. Phys. 42 (2009) 155107(1)–155107(6).
[28] X.P. Yan, Q. Liu, H.L. Chen, F. Xing, M.L. Gong, D.S. Wang, A novel orthogonally linearly polarized Nd:YVO_4 laser, Chin. Phys. B 19 (2010) 084202(1)–084202(6).
[29] B. Wu, P. Jiang, D. Yang, T. Chen, J. Kong, Y. Shen, Compact dual-wavelength Nd:$GdVO_4$ laser working at 1063 and 1065 nm, Opt. Express 17 (2009) 6004–6009.
[30] Y. Lü, P. Zhai, J. Xia, X. Fu, S. Li, Simultaneous orthogonal polarized dual-wavelength continuous-wave laser operation at 1079.5 nm and 1064.5 nm in Nd:$YAlO_3$ and their sum-frequency mixing, J. Opt. Soc. Am. B 29 (2012) 2352–2356.
[31] Y.P. Huang, C.Y. Cho, Y.J. Huang, Y.F. Chen, Orthogonally polarized dual-wavelength Nd:$LuVO_4$ laser at 1086 nm and 1089 nm, Opt. Express 20 (2012) 5644–5651.
[32] W. Shi, Y.J. Ding, N. Fernelius, K. Vodopyanov, Efficient, tunable, and coherent 0.18–5.27 T Hz source based on GaSe crystal, Opt. Lett. 27 (2002) 1454–1456.
[33] J.F. Federici, B. Schulkin, F. Huang, D. Gary, R. Barat, F. Oliveira, D. Zimdars, THz imaging and sensing for security applications—explosives, weapons and drugs, Semicond. Sci. Technol. 20 (2005) S266–S280.
[34] J.B. Baxter, G.W. Guglietta, Terahertz spectroscopy, Anal. Chem. 83 (2011) 4342–4368.
[35] C.B. Reid, E. Pickwell-MacPherson, J.G. Laufer, A.P. Gibson, J.C. Hebden, V.P. Wallace, Accuracy and resolution of THz reflection spectroscopy for medical imaging, Phys. Med Biol. 55 (2010) 4825–4838.
[36] L. Fei, S. Zhang, The discovery of nanometer fringes in laser self-mixing interference, Opt. Commun. 273 (2007) 226–230.
[37] S. Zhang, Y. Tan, Y. Li, Orthogonally polarized dual frequency lasers and applications in self-sensing metrology, 21, 2010, pp. 054016(1)-054016(9)
[38] Y. Lü, X. Zhang, A. Zhang, X. Yin, J. Xia, Efficient 1047 nm CW laser emission of Nd:YLF under direct pumping into the emitting level, 283, 2010, pp. 1877–1879
[39] G. Cerullo, S. De Silvestri, V. Magni, High efficiency, 40 W cw Nd:YLF laser with large TEM_{00} mode, Opt. Commun. 93 (1992) 77–81.
[40] B. Frei, J.E. Balmer, 1053 nm-wavelength selection in a diode-laser-pumped Nd:YLF laser, Appl. Opt. 33 (1994) 6942–6946.
[41] Y. Sun, H. Zhang, Q. Liu, L. Huang, Y. Wang, M. Gong, High pulse repetition frequency all-solid-state 1053 nm Nd:YLF laser, Laser Phys. Lett. 7 (2010) 722–725.
[42] Y.F. Lü, J. Xia, X.H. Zhang, A.F. Zhang, J.G. Wang, L. Bao, X.D. Yin, High-efficiency direct-pumped Nd:YLF laser operating at 1321 nm, Appl. Phys. B. 98 (2010) 305–309.
[43] F. Balembois, D. Boutard, E. Barnasson, M. Baudrier, R. Pariès, C. Schwach, S. Forget, Efficient diode-pumped intracavity frequency-doubled CW Nd:YLF laser emitting in the red, Opt. Laser Technol. 38 (2006) 626–630.
[44] C.L. Li, X.H. Zhang, W. Liang, Z.M. Zhao, Diode-pumped continuous-wave Nd:YLF laser at 1313 nm, Laser Phys. 21 (2011) 340–342.
[45] Y. Louyer, F. Balembois, M.D. Plimmer, T. Badr, P. Georges, P. Juncar, M.E. Himbert, Efficient cw operation of diode-pumped Nd:YLF lasers at 1312.0 and 1322.6 nm for a silver atom optical clock, Opt. Commun. 217 (2003) 357–362.
[46] Y.V. Pruneri, R. Koch, P.G. Kazansky, W.A. Clarkson, P. St.J. Russell, D.C. Hanna, 49 mW of cw blue light generated by first-order quasi-phase-matched frequency doubling of a diode-pumped 946 nm Nd:YAG laser, Opt. Lett. 20 (1995) 2375–2377.
[47] S. Spiekermann, F. Laurell, Continuous wave and Q-switched operation of diode pumped quasi-three level Nd:YLF lasers, Adv. Solid State Lasers Opt. Soc. Am. (2000).
[48] Y. Lü, X. Zhang, W. Cheng, J. Xia, All-solid-state cw frequency-doubling Nd:$YLiF_4$/LBO blue laser with 4.33 W output power at 454 nm under in-band diode pumping at 880 nm, Appl. Opt. 49 (2010) 4096–4099.
[49] W. Liang, X.H. Zhang, Z.L. Liang, Y.Q. Liu, Z. Liang, Efficient continuous-wave 908 nm Nd:YLF laser emission under direct 880 nm pumping, Laser Phys. 21 (2011) 320–322.
[50] D. Geskus, Neto J. Jakutis, N.U. Wetter, Experimental analysis of quasi three level Nd:YLF laser operating at 908 nm with a peak output power of 6.4 W, Adv. Solid State Lasers Opt. Soc. Am. (2013).
[51] T.Y. Fan, R.L. Byer, Diode laser-pumped solid-state lasers, IEEE J. Quantum Electron. 24 (1998) 895–912.
[52] D. Findlay, R.A. Clay, The measurement of internal losses in 4-level lasers, Phys. Lett. 20 (1966) 277–278.